FACTA UNIVERSITATIS
Series: **Mechanical Engineering**
https://doi.org/10.22190/FUME240414028W

Original scientific paper

INFLUENCE OF TANGENTIAL SLIDING ON THE CONTACT AREA OF A MACROSCOPIC ADHESIVE CONTACT

Josefine Wilhayn, Iakov A. Lyashenko, Qiang Li, Valentin L. Popov

Department of System Dynamics and Friction Physics, Technische Universität Berlin, Berlin, Germany

Abstract. *Influence of tangential force on the adhesive contact, in particular on the adhesive strength and the contact area have been a subject of investigation and discussions for many years. Depending on the system under consideration, both increase and decrease of adhesion strength due to shearing of an adhesive contact have been reported. The same is valid for change of the contact area. While it is generally accepted that the contact area decreases when applying tangential traction, also opposite behaviour is possible. In the present paper we study theoretically and experimentally the conditions under which the contact area may increase or decrease due to shear.*

Key words: *Adhesion, Contact area, Shear, Tangential loading*

1. INTRODUCTION

Influence of tangential traction and shear on adhesive contacts has been subject of interest both from the viewpoint of fundamental contact mechanics [1][2] and biological applications as gecko feet [3]. One of the problems in the discussion of adhesive contacts under shear is that it is assumed that the term "adhesive contact" is well defined. In reality, the concept of adhesive contact can hide systems of different physical nature. Adhesive contact can mean a "glued" contact, which may be destroyed by both normal and tangential movement of contacting bodies. In this case, the combined energy release rate can be defined as it was done in [1] or [4]. The same approach based on the energy release rate is used in the paper [5] for analyzing contact area between a glass plate and PDMS bar where an intermediate situation is realized (both sticking and sliding are possible). The adhesive contact described in the classical theory by Johnson, Kendall and Roberts (JKR) [6] is, on the contrary, of completely different nature. One of assumptions of the JKR theory is the absence of friction. According to JKR, shearing of an adhesive contact does not lead to appearance of tangential force and does not influence any properties of the adhesive contact. This contradicts observations of real adhesive contacts.

Received: April 14, 2024 / Accepted May 17, 2024
Corresponding author: Valentin L. Popov
Technische Universität Berlin, Sekr. C8-4, Straße des 17. Juni 135, D-10623 Berlin
E-mail: v.popov@tu-berlin.de

However, the JKR theory illustrates that the presence of any kind of friction is by no means a necessary, intrinsic property of adhesive contacts. At least in the model, one can imagine contacts without friction. This is e.g. the case of two absolutely smooth surfaces interacting by van der Waals forces as described in the Lifshitz's theory [7]. In the present paper, we will discuss a model very closely related to the (frictionless) JKR model but with consideration of surface roughness or surface profiling. We will show that already this model exhibits all basic properties of adhesive contacts which are observed experimentally. In particular, it shows adhesion hysteresis during all stages of indenting and detaching. The existence of the adhesive hysteresis which was observed experimentally and described theoretically in different context in [8-12], means that the state of adhesive contact is not unique but does depend on the prehistory of loading. We will show that this prehistory influences essentially the interplay of normal and tangential loadings.

2. Adhesion Hysteresis in Frictionless Profiled Contact

The simplest model of an adhesive contact of bodies with rough (or profiled) surfaces was considered by Fuller and Tabor [13]. We will use this model in an even more simplified form described in [14]. Instead of a continuous smooth surface, a set of individual asperities is considered. The main physical difference from the case of smooth surfaces is that the surface profile prevents propagation of the adhesive contact (which is essentially the Griffith's crack [15]). We will be interested in the macroscopic contacts between a flat and a parabolically shaped bodies, so the individual independent asperities will be placed on the same level. For illustration, we consider asperities as springs of equal stiffness (Fig. 1), however, the true three-dimensional distribution of stresses is considered below in numerical simulation.

The model presented in Fig. 1 exhibits pronounced adhesion hysteresis. The starting no-contact position of indenter is shown in Fig. 1a. When it comes in touch with the substrate and indents further (Fig. 1b), only the springs (summits, asperities) come into contact which correspond to the geometrical intersection of the profiles of contacting bodies. The adhesion does not play any role at the stage of indentation, so the behavior is identical with that of a non-adhesive contact. If we would consider elastic interrelation of asperities, we would become pure Hertzian behavior [16]. At the stage of pull-off (Fig. 1c), the springs which came into contact during indentation will first follow the indenter until they do not reach some critical elongation. Thus, the system behaves as an adhesive contact. If as detachment criterion the Heß's criterion is used, then the resulting force-displacement curve will coincide with that of the JKR theory [17]. Our experiments described in [11] exhibit exactly such behavior: practically pure Hertzian indentation (with only very minor jump into contact), and strong JKR-adhesion during detaching. Note that this hysteresis is not connected with any frictional forces in the interface, as we consider here frictionless adhesive contact, but solely with preventing interfacial crack propagation due to surface profile (or roughness).

To retain the model as simple as possible, we will neglect in the following the frictional force in the interface. We thus assume that any individual spring can slide frictionless along the surface of the counter body (as JKR-contact does).

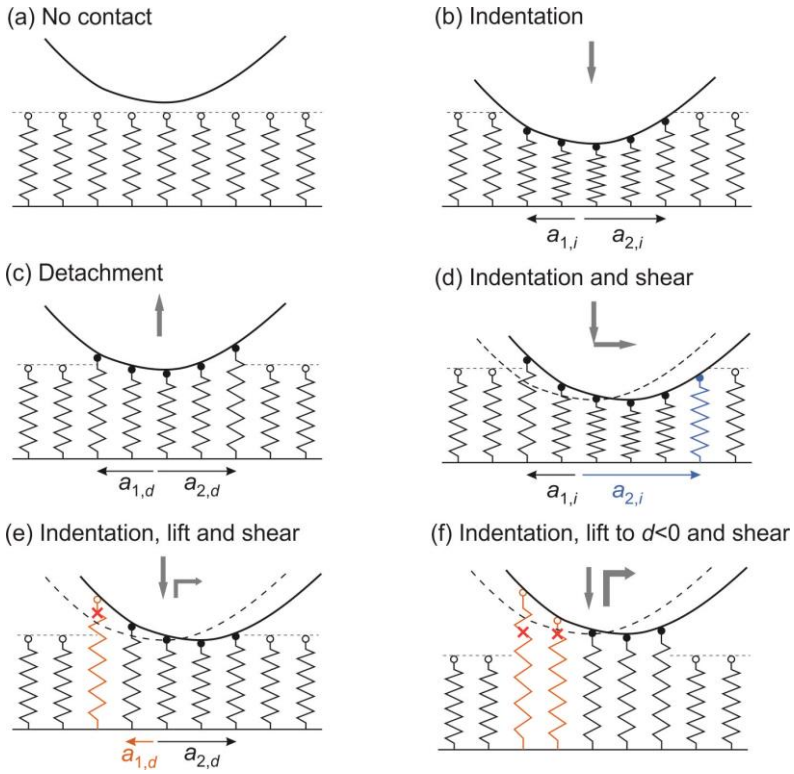

Fig. 1 Illustration of indentation, pull-off and tangential sliding of an indenter on an elastic substrate. (a)-(c) show indentation and pull-off, (d) sliding after indentation, (e) sliding after indentation and lifting, (f) similar to (e) but lifting to a negative depth.

We start with a detailed discussion of the normal contact problem. If a rigid indenter is pressed into an elastomer to some depth, and then the movement is reversed, then there will be a phase when the contact area does not change (until the edge springs achieve a critical elongation). This leads to appearance of a linear part of the force-displacement relation. After arriving at this critical value, the force follows the curve for an adhesive contact. Let us now consider two cases:

I. *The indenter is monotonically pressed into the elastic counter body, stopped, and then moved tangentially at the achieved indentation* (Fig. 1d). Note that each individual spring is assumed to have a frictionless contact with the indenter. This means, that the springs freely can slide along the indenter. If we move the indenter by one spacing between springs, the last spring on the leading edge will be pressed down, and the indenter will come into contact with the next spring. This means that the leading edge will move in the direction of the movement of indenter with the same velocity. The spring at the trailing edge, on the contrary, will move upwards (by sliding along the profile of the indenter), and thus will remain at the same place. This means that the contact area will become larger at the leading half of the contact area and remain at place at the training part, thus the contact area will increase, and the contact area becomes elongated in the direction of movement.

As soon as the edge spring at the trailing edge achieves the critical elongation, the trailing boundary starts moving together with the indenter and the contact area remains constant.

II. *The indenter is pressed into the elastic counter body, then lifted to the end of the plateau of the contact area, and only then moved tangentially* (Fig. 1e). Lifting to the end of the plateau means that now the edge springs are already in the critical state. If we now move the indenter to the right, the springs at the leading edge will first be pressed down, and the boundary on the leading edge will remain at place. On the trailing edge, on the contrary, the springs were already in the critical state. They will slide up the profile and detach immediately. This means, that the trailing edge will move forward (in the same direction as indenter and with the same velocity). Thus, the contact area will decrease and will become elongated in the direction perpendicular to the direction of sliding.

III. *The indenter is pressed into the elastic counter body, then lifted to the zero or negative indentation depth, and then moved tangentially* (Fig. 1f). Note that if the indenter is pulled off to the zero or moderate negative indentation depth in the normal direction, the adhesive contact is still not destroyed, and the edge springs are in the critical state, so that the initial state is very similar to that of the case II. Tangential movement of the indenter will lead to pressing down the springs on the leading edge and detaching of springs on the trailing edge. This means that the leading edge will remain at place. However, now no new springs will come into contact because of the negative indentation depth. At the same time, the trailing edge will move forward together with the indenter. The contact area will shrink until it disappears completely.

Experiments described in [11] confirm qualitatively the existence of the above described three different cases. However, the scenarios described above present only a very rough zero-order "impressionist" picture of how the prehistory of loading influences the reaction of the system to shear. The model used has a number of assumptions which are not valid for real systems and will influence the details of happening. This is in particular the assumption of frictionless contact for each individual asperity. Experiments show that much better assumption is existence of a constant shear stress which has to be overcome to move an asperity [11]. We further assumed that the detachment condition of an individual spring is constant. In reality it is a function of the whole contact configuration. Finally, non-linear effects may come into play making the behavior very complicated [18].

3. EXPERIMENT

In our experiments, a spherical indenter with a radius R = 100 mm was pressed into a layer of elastomer with a thickness h = 5 mm to a depth of d_{max} = 0.3 mm, then either lifted to different indentation depth until complete disappearance of contact, and subsequently shifted in the tangential direction. A photo of the setup is shown in Fig. 2. The detailed description of the experimental setup is provided in the previous work [19].

The indenter was moved at a velocity of v =3 μm/s throughout all phases of indentation, pull-off and shearing. At such low velocity, the contact can be considered as quasi-static, and viscosity can be neglected. We conducted experiments with two types of elastomers – a softer TANAC CRG N0505, and a harder TANAC CRG N3005.

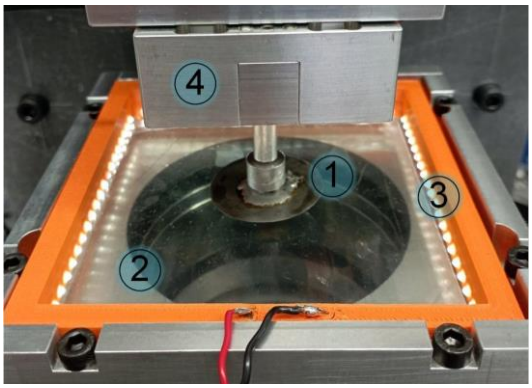

Fig. 2 View of the experiment setup: 1 − steel indenter with a radius of R = 100 mm; 2 − a sheet of elastomer placed on a solid glass plate; 3 − an omnidirectional LED lighting; 4 − force sensor for measuring all three components of the contact force.

3.1 Indentation in Softer Material TANAC CRG N0505

Fig. 3 illustrates the dependencies of the normal force F_N and the contact area A on the indentation depth d during the indentation into the softer material CRG N0505.

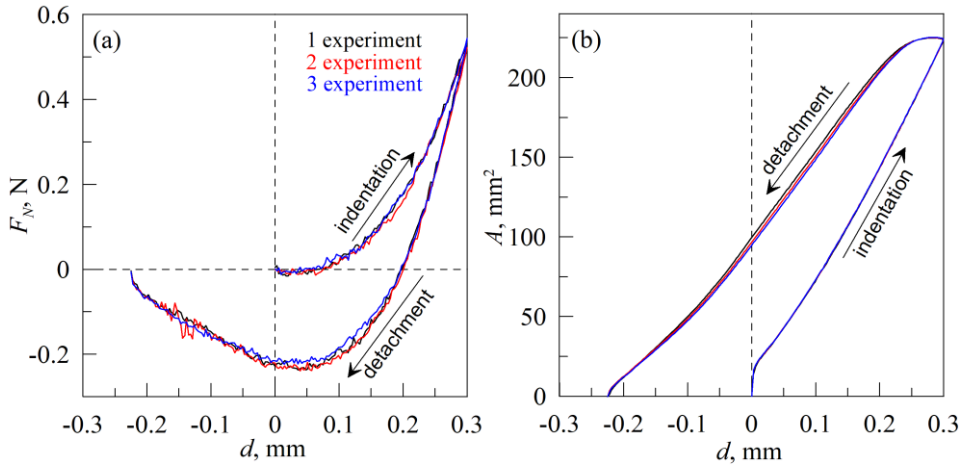

Fig. 3 The dependencies of the normal force F_N (a) and the contact area A (b) on the indentation depth d during the indentation of an indenter with a radius R = 100 mm into a layer of elastomer TANAC CRG N0505 with a thickness h = 5 mm. The figure shows the results of three consecutive cycles of indentation/detachment.

One can see that there is a small jump-like increase in contact area at the point of initial contact, after which the area A increases linearly with further indentation. When the direction of the indenter motion is changed towards withdrawal, the contact area remains constant for some period of time before it starts decreasing. While the contact area remains constant, a constant contact stiffness $K = \partial F_N/\partial d$ is realized, hence immediately after

changing the direction of motion, a linear segment of the force dependence $F_N(d)$ is observed. Fig. 3 demonstrates the results of three consecutive experiments, with curves on both panels of the figure overlapping, indicating the repeatability of the experiments. Therefore, in the experiments on tangential contact, only one experiment will be conducted for each loading scenario.

The results of a series of experiments on tangential loading of the contact are shown in Fig. 4. Here, in all experiments, the indenter was first immersed into the elastomer to the maximum depth $d = d_{max} = 0.3$ mm, then lifted to a smaller value $d = d_0$, and subsequently shifted tangentially by a distance $x = 1$ mm at a fixed value of indentation depth $d = d_0$. Vertical lines on all panels of the figure denote the moments of the start of tangential displacement of the indenter in all 4 experiments with different values of d_0.

In the first experiment, the tangential displacement of the indenter was carried out immediately after reaching the depth d_{max}, i.e., in this experiment $d_0 = d_{max}$. This corresponds to the case I of Section 2. As seen in Fig. 4a, the normal force remains close to that corresponding to the maximum indentation depth after the start of tangential displacement, while the tangential force begins to increase. Fig. 4b shows the coordinates of the leading and trailing edges of the contact zone. Additionally, for clarity, dashed lines close to horizontal are shown on Fig. 4b, representing straight lines defined by equations

$$Coordinate = B + 0.18t\,. \tag{1}$$

Here, the coefficient 0.18 corresponds to the velocity of the indenter motion $v = 3$ μm/s. If the edges of the contact were moving exactly at the speed of the indenter after the start of its tangential motion, the experimental dependencies shown in Fig. 4b would coincide with these dashed lines. However, upon closer examination of the experimental dependencies, it can be observed that immediately after the start of tangential motion, only the trailing edge of the contact moves at the speed of the indenter, which occurs in the time interval $t = 1.65 – 3.1$ min. The leading edge of the contact begins to move at a speed slightly exceeding the speed of the indenter. This indicates the spreading of the contact at the leading edge after the start of tangential motion, as well as the fact that the contact boundary moves together with the indenter at the trailing edge. However, the situation changes at times $t > 3.1$ min, when contact failure begins at the trailing edge, while at the leading edge, its propagation continues as before. The basic features of this behavior: a more rapid propagation of the leading edge of the contact and increase of the contact area are the same as predicted by the simple model (Section 2, case I). Different from prediction, the rear edge does first slowly move together with indenter (which might relate to final interfacial friction contrary to the model). As predicted, after achieving some critical position, it accelerates but moves faster than the indenter, which may be related with the assumption of independent springs (which is not valid in the real system). The main conclusion of theory remains valid: If tangential loading occurs at the position of maximum indentation, then the contact area increases due to shear.

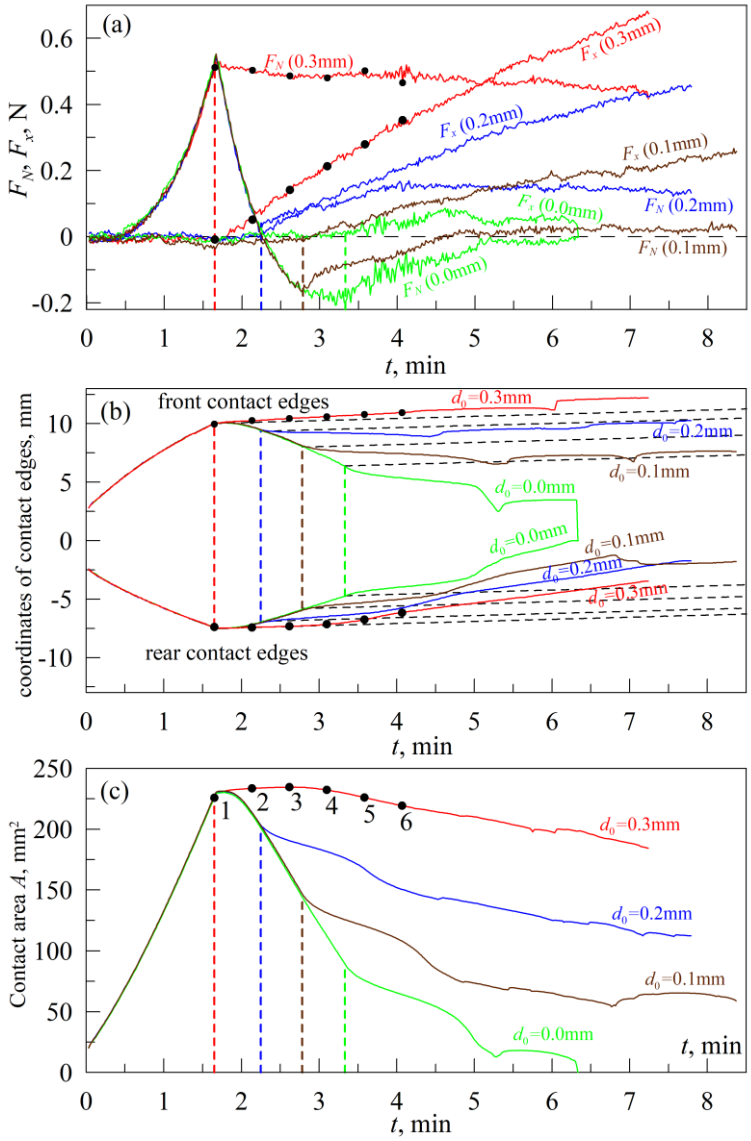

Fig. 4 The dependencies of the normal F_N and tangential F_x contact forces (a), coordinates of the leading and trailing contact edges (b), and the contact area A (c) on the experiment time t during indentation into the softer material CRG N0505.

Behavior after some initial lift also qualitatively corresponds to that described in Section 2. In particular, at the zero indentation depth the contact finally disappears completely.

To provide a more detailed understanding of the contact spreading characteristics after the start of the indenter motion, we additionally present Fig. 5. This figure shows contact

photographs corresponding to six consecutive states, which are shown on all panels in Fig. 4. These states are separated by equal time intervals. In addition to the contact photographs, the left panel of Fig. 5 shows profiles of the contact boundary, which allow easy tracking of the evolution of the contact boundary spreading. The results confirm the conclusions made above. Specifically, the first four contact configurations demonstrate the spreading of the contact at its leading edge, while the contact boundary at the trailing edge remains almost stationary. However, the subsequent configurations 5 and 6 show a faster displacement of the contact boundary at the trailing edge, while the spreading characteristics of the contact remain unchanged at the leading edge.

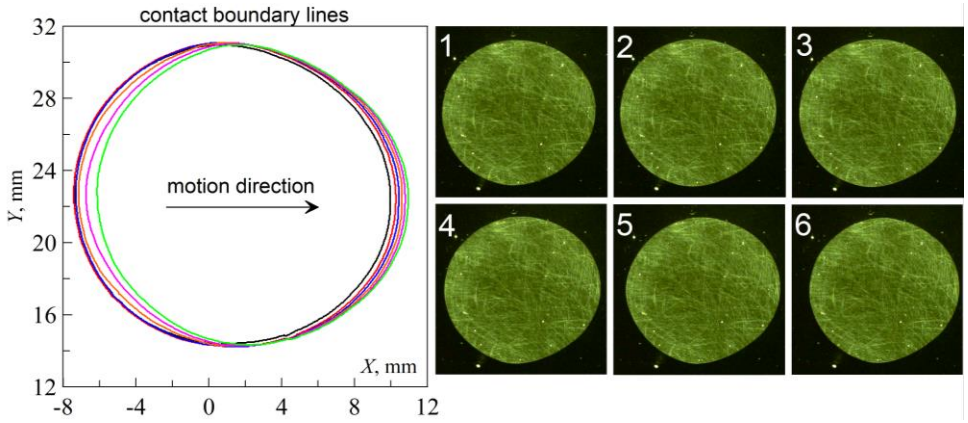

Fig. 5 Right panel – photographs of the contact area corresponding to points 1–6 in Fig. 4. Left panel – contact boundaries corresponding to the photographs in the right panel. Experiment on indentation into the softer material CRG N0505 is shown.

Let's go back to Fig. 4 and look at forces. If indenter is pressed into counter body and then immediately moved tangentially, then, the contact configuration on the leading edge will not change essentially, but the springs on the rear edge will slide up, so that attractive part of the contact force will increase. This means decreasing of the total normal force. This is exactly what is observed in experiment (Fig. 4a, red curve corresponding to indentation 0.3 mm). If, however, the indenter is pressed into the counter body and then lifted at last to the end of the plateau of the contact area (blue, brawn and green curves in Fig. 4a), then the contact situation on the rear end will not change while at the front edge the springs will glide downwards and so the normal force will increase. This behavior is observed in experiment.

3.2 Indentation in Hard Material TANAC CRG N3005

We would like to stress that this behavior is universal. A set of experiments conducted with rubber TANAC CRG N3005 which is 10 times stiffer than the previous one show very similar results with the main difference that the forces are scaled by the factor of 10 (Fig. 6). Interestingly, this scaling is equal both to normal and tangential forces indicating that the tangential force strongly correlates with the adhesion force, as it should be accordingly to the model described in Section 2.

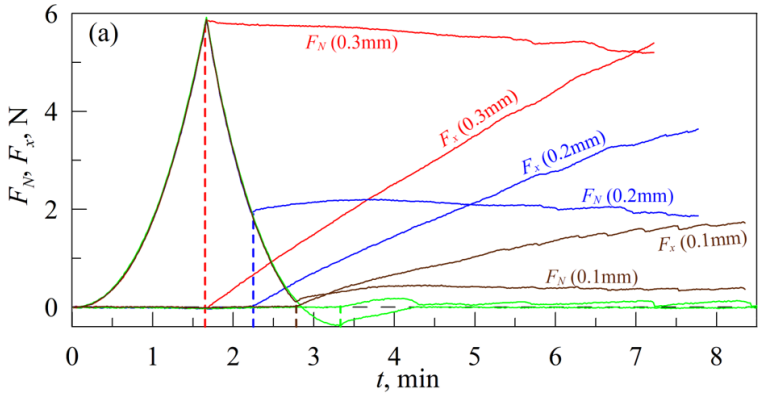

Fig. 6 Dependences of normal F_N and tangential F_x forces on the time of experiment t during indentation into the softer material CRG N3005. The lower curves corresponding to the depth d_0 = 0.0 mm are not labelled.

4. Numerical Simulation

Numerical simulation was carried out using the Boundary Element Method for JKR-type adhesive contacts [20, 21]. We consider a rough sphere in contact with an elastic rough substrate. The geometry of the rough sphere is modeled by a parabolic profile superposed with a two-dimensional waviness. The surface of elastic substrate is also a two-dimensional waviness with the same amplitude δ and wave length λ, but rotated in plane by an angle $\pi/8$. The amplitude and wavelength are much smaller than the sphere radius, δ/λ =0.028, and λ/R = 0.005. The following results are normalized by the JKR-solution for smooth sphere [6]

$$|F_{\mathrm{JKR}}| = \frac{3}{2}\pi\gamma R\,,\ |d_{\mathrm{JKR}}| = \left(\frac{3\pi^2\gamma^2 R}{64E^*}\right)^{1/3},\ |a_{\mathrm{JKR}}| = \left(\frac{9\pi\gamma R^2}{8E^*}\right)^{1/3}. \qquad (2)$$

Here γ is the work of adhesion per unit area, and E^* is the effective elastic modulus. In the following we first show the simulation of a whole indentation process including both indenting and pull-off, then the sliding contact corresponding to cases I and II in section 2.

4.1 Simulation of Indentation Test

Fig. 7 shows simulation of an indentation test: indenter is brought into contact (position 1) and pressed to the position 3 (with indentation depth d=6$|d_{\mathrm{JKR}}|$), then it is lifted until it is completely detached. Due to roughness, the curves for indenting and pull-off do not coincide with the analytical JKR-solution for smooth sphere (gray lines), and the adhesion hysteresis can be clearly observed. Note that after indenting to position 3, when the movement direction changes from indenting to pull-off, the contact area remains unchanged up to position 4, well seen in contact area-normal force relation in Fig. 7b and from contact areas shown in Fig. 7c. This behavior is also described in experiment in Fig. 3. The mean contact radius in following figures is defined as a=$(A_{\mathrm{con}}/\pi)^{1/2}$.

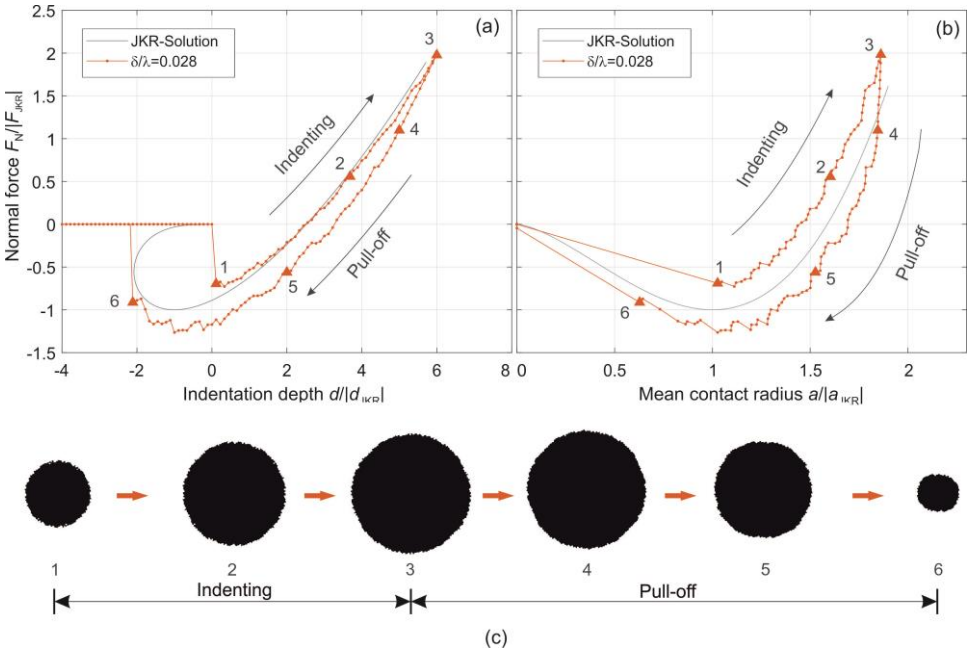

Fig. 7 Simulation of indenting and pull-off of a rigid rough sphere in contact with an elastic rough substrate. Dependence of the normal force on indentation depth (a) and mean contact radius (b). Figure (c) shows contact area changing during the whole process.

4.2 Simulation of Sliding

Based on the normal contact in Fig. 7, we consider two sliding cases: (1) the indenter is pressed into position 3, then it moves tangentially; (2) the indenter is pressed to the position 3, lifted to the position 4 (the contact area remains unchanged during this stage), then the indenter slides tangentially. We focus on the change in contact area during the sliding process. Indentation depth keeps constant during sliding.

Fig. 8a presents the dependence of the mean contact radius on the sliding distance. The contact area increases during the sliding. The first image in Fig.8b is the contact area when the indenter is pressed to position 3. The blue color in second and third images represents the increased area in comparison with state 3, and the orange color represents the reduced area. One can clearly see the enlargement of contact region after sliding. It occurs at the rear edge as explained in Section 2, case I. Fig.8c and Fig.8d show the normal force decreasing during the sliding and the dependence of tangential force on the sliding distance.

Fig. 9 shows the case of sliding after indentation and pull-off to position 4. The first image in Fig. 9b shows the contact area when the indenter is pulled off to position 4. From both curve in Fig. 9a and images of contact area, it is seen that the contact area is reduced during sliding in this case. These results agree with the prediction in Section 2.

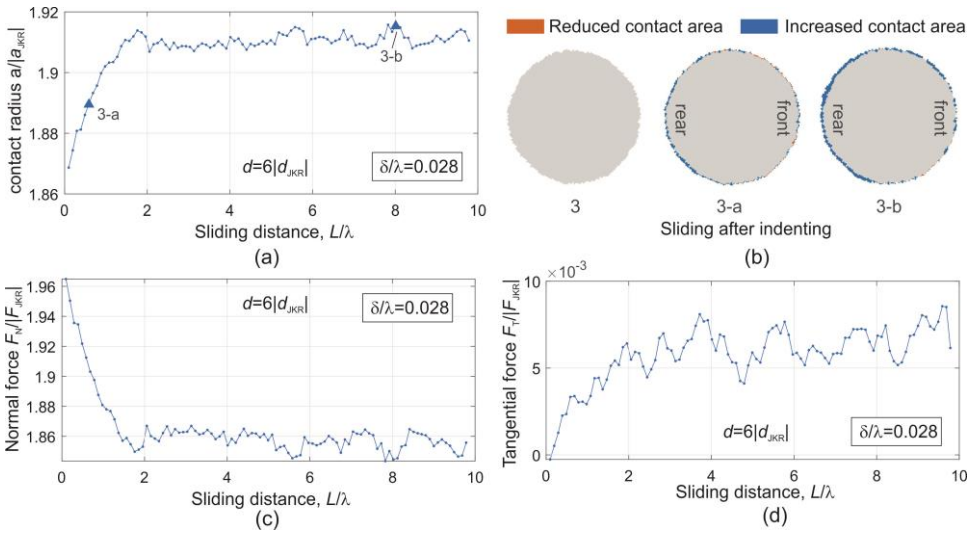

Fig. 8 Sliding after indenting to position "3" shown in Fig.7. (a) Mean contact radius as function of sliding distance. (b) Images of contact area. The first image corresponds to the point 3 in Fig.7c. Images 3-a and 3-b are contact areas when sliding. Orange color represents the area lost compared to state "3" and blue color represents the increased area. (c) Dependence of normal force and (d) tangential force on sliding distance.

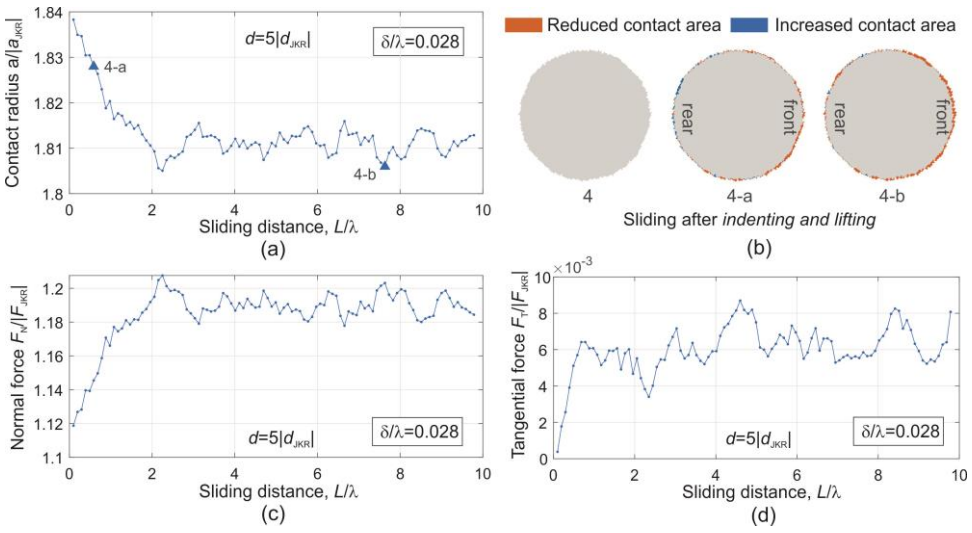

Fig. 9 Sliding after *indenting and pull-off* to position "4" shown in Fig.7. (a) Mean contact radius changing during the sliding. (b) Images of contact area during sliding. (c) Dependence of normal force and (d) tangential force on sliding distance.

5. CONCLUSIONS

Analysis of experimental data on shearing adhesive contacts after pre-loading shows that the reaction of the contact on shear does depend on the preloading history. Depending on preloading, shear can lead to increase or decrease of contact area and to decrease or increase of normal contact force. A very rough understanding of all possible situations is provided already by a very simple model based on Fuller and Tabor model. More detailed understanding can be achieved by considering correct three-dimensional stress distribution (e.g. using BEM simulation). Numerical simulations show smaller effects of area increase and decrease depending as in experiment. This discrepancy may be caused by relaxation effects. The complete understanding probably needs consideration of material and geometrical non-linearities.

Acknowledgement: *This work has been conducted under financial support from the Deutsche Forschungsgemeinschaft (DFG Grant numbers PO 810/55-3 and LI 3064/2-1).*

REFERENCES

1. Johnson, K.L., 1997, *Adhesion and friction between a smooth elastic spherical asperity and a plane surface*, Proceedings of the Royal Society of London. Series A, Mathematical and Physical Sciences, 453, pp. 163–179.
2. Ciavarella, M., McMeeking, R.M., Cricrì, G., 2023, *On the afferrante-carbone theory of ultratough tape peeling*, Facta Univesitatis-Series Mechanical Engineering, 21(4), pp. 727-735.
3. Tian, Y., Pesika, N., Zeng, H., Rosenberg, K., Zhao, B., McGuiggan, P., Autumn, K., Israelachvili, J., 2006, *Adhesion and friction in gecko toe attachment and detachment*, Proceedings of the National Academy of Sciences, 103(51), pp. 19320-19325.
4. Popov, V.L., Lyashenko, I.A., Filippov, A.E., 2017, *Influence of tangential displacement on the adhesion strength of a contact between a parabolic profile and an elastic half-space*, Royal Society Open Science, 4(8), 161010.
5. Sahli, R., Pallares, G., Papangelo, A., Ciavarella, M., Ducottet, C., Ponthus, N., Scheibert, J., 2019, *Shear-induced anisotropy in rough elastomer contact*, Physical Review Letters, 122, 214301.
6. Johnson, K.L., Kendall, K., Roberts, A.D., 1971, *Surface Energy and the Contact of Elastic Solids*, Proceedings of the Royal Society of London. Series A, Mathematical and Physical Sciences, 324, pp. 301–313.
7. Lifshitz, E.M., 1956, *The theory of molecular attractive forces between solids*, Soviet Physics JEPT, 2, pp. 73-83.
8. Chaudhury, M.K., Owen, M.J., 1993, *Adhesion hysteresis and friction*, Langmuir, 9(1), pp. 29–31.
9. Nosonovsky, M., 2007, *Model for solid-liquid and solid-solid friction of rough surfaces with adhesion hysteresis*, The Journal of Chemical Physics, 126, 224701.
10. Müller, Ch., Samri, M., Hensel, R., Arzt, E., Müser, M.H., 2023, *Revealing the coaction of viscous and multi-stability hysteresis in an adhesive, nominally flat punch: A combined numerical and experimental study*, Journal of the Mechanics and Physics of Solids, 174, 105260.
11. Popov, V.L., Li, Q., Lyashenko, I.A., Pohrt, R., 2021, *Adhesion and friction in hard and soft contacts: theory and experiment*, Friction, 9, pp. 1688–1706.
12. Sanner, A., Kumar, N., Dhinojwala, A., Jacobs, T.D.B., Pastewka, L., 2024, *Why soft contacts are stickier when breaking than when making them*, Science Advances, 10(10), eadl1277.
13. Fuller, K.N.G., Tabor, D., 1975, *The effect of surface roughness on the adhesion of elastic solids*, Proceedings of the Royal Society of London. Series A, Mathematical and Physical Sciences, 345, pp. 327–342.
14. Popov, V.L., 2017, *Contact Mechanics and Friction: Physical Principles and Applications*, Springer, Berlin, 391 p.
15. Tserpes, K., Barroso-Caro, A., Carraro, P.A., Beber, V.C., Floros, I., Gamon, W., Kozłowski, M., Santandrea, F., Shahverdi, M., Skejić, D., Bedon, C., Rajčić, V., 2022, *A review on failure theories and simulation models for adhesive joints*, The Journal of Adhesion, 98(12), pp. 1855–1915.

16. Barber, J.R., 2018, *Contact Mechanics*, Springer Cham, 585 p.
17. Heß, M., 2012, *On the reduction method of dimensionality: The exact mapping of axisymmetric contact problems with and without adhesion*, Physical Mesomechanics, 15(5), pp. 264-269.
18. Mergel, J.C., Scheibert, J., Sauer, R.A., 2021, *Contact with coupled adhesion and friction: Computational framework, applications, and new insights*, Journal of the Mechanics and Physics of Solids, 146, 104194.
19. Lyashenko, I.A., Pham, T.H., Popov, V.L., 2024, *Effect of Indentation Depth on Friction Coefficient in Adhesive Contacts: Experiment and Simulation*, Biomimetics, 9, 52.
20. Popov, V.L., Pohrt, R., Li, Q., 2017, *Strength of adhesive contacts: Influence of contact geometry and material gradients*, Friction, 5, pp. 308–325.
21. Wang, Q.J., Sun, L., Zhang, X., Liu, S., Zhu, D., 2020, *FFT-Based methods for computational contact mechanics*, Frontiers in Mechanical Engineering, 6, 61.